4690 *Chem. Mater.* **2010,** *22,* 4690–4699
DOI:10.1021/cm100969n

CHEMISTRY OF MATERIALS
Article

Phase Stability and Superconducting Properties of AlB_2-Type $YbGa_xSi_{2-x}$ ($1.12 \leq x \leq 1.49$)

Naohito Tsujii,*[,†] Motoharu Imai,[†] Hitoshi Yamaoka,[‡] Ignace Jarrige,[§] Hirofumi Oohashi,[∥] Tatsunori Tochio,[⊥] Katsumi Handa,[#] Junko Ide,[#] Hideki Atsuta,[#] Yoshiaki Ito,[#] Hideki Yoshikawa,[∥] and Hideaki Kitazawa[†]

[†]*National Institute for Materials Science, 1-2-1 Sengen, Tsukuba 305-0047, Japan,* [‡]*Harima Institute, RIKEN (The Institute of Physical and Chemical Research), Sayo, Hyogo 679-5148, Japan,* [§]*Synchrotron Radiation Research Center, Japan Atomic Energy Agency, 1-1-1 Kouto, Sayo, Hyogo 679-5148, Japan,* [∥]*Beamline Station, National Institute for Materials Science, 1-1-1 Kouto, Sayo, Hyogo 679-5148, Japan,* [⊥]*Department of Physics, Kobe University, Kobe 657-8501, Japan, and* [#]*Institute for Chemical Research, Kyoto University, Uji, Kyoto 611-0011, Japan*

Received April 8, 2010. Revised Manuscript Received July 6, 2010

We investigated the phase stability and superconducting properties of $YbGa_xSi_{2-x}$. Polycrystalline samples were synthesized by argon arc melting and subsequent annealing. The composition range of the phase with the AlB_2-type structure was determined to be $1.12(1) \leq x \leq 1.49(3)$ by powder X-ray diffraction and electron probe microanalysis. The lattice constants, both a and c, increase linearly with x throughout the single-phased region. Electrical resistivity showed metallic behavior for all samples, and the superconducting transition was observed to occur at critical temperatures ranging from $T_C = 2.4$ K for $x = 1.15$ to less than 1.8 K for $x = 1.41$. The extent of the decrease in T_C with x is comparable to that in MGa_xSi_{2-x} (M = Ca, Sr, Ba) for $x > 1$. The negative sign of the Seebeck coefficient measured for $x = 1.20$ indicates that the dominant carriers are electrons. The temperature dependence of the magnetic susceptibility below room temperature showed almost nonmagnetic behavior suggesting the nearly divalent state of Yb. However, Yb was found to be in the mixed valent state $Yb^{2.3+}$ based on a precise measurement using X-ray absorption spectroscopy in the partial fluorescence yield mode at the Yb L_{III} absorption edge. Comparison is made with the nonsuperconducting YbGaGe from the viewpoint of the relation of the crystal structure and superconductivity.

Introduction

The discovery of superconductivity in MgB_2 below $T_C = 39$ K triggered extensive research for new superconductors with the AlB_2-type structure.[1] Thus, ternary silicides with the AlB_2-type structure, MAl_xSi_{2-x} and MGa_xSi_{2-x} (M = Ca, Sr, Ba), have been found to show superconductivity.[2−9] The AlB_2-type structure is illustrated in Figure 1a. In those ternary silicides, the honeycomb layers composed of Si and Al/Ga are stacked along the c-axis, with alkaline earth atoms intercalated in between. In spite of the structural similarity with MgB_2, the electronic structure of the ternary silicides was found to differ significantly from that of MgB_2. Carriers responsible for superconductivity for MgB_2 are holes in the highly 2-dimentional sigma band derived from the boron layer.[10] In contrast, dominant carriers in the ternary silicides are electrons as suggested by negative Seebeck coeffient for (Ca,Sr)AlSi and SrGaSi[7,8] and by the Hall effect measurements for CaAlSi.[11] Band calculations suggested that the hybridized band formed from the d orbital of the alkaline earth atoms and the p orbitals of the Al/Ga and Si atoms plays an essential role in the superconductivity,[2,12−16] meaning that the superconductivity has a 3-dimensional character.

*To whom correspondence should be addressed. Tel.: +81-29-859-2817. Fax: +81-29-859-2801. E-mail: TSUJII.Naohito@nims.go.jp.

(1) Nagamatsu, J.; Nakagawa, N.; Muranaka, T.; Zenitani, Y.; Akimitsu, J. *Nature* **2001**, *410*, 63.
(2) Imai, M.; Abe, E.; Ye, J.; Nishida, K.; Kimura, T.; Honma, K; Abe, H.; Kitazawa, H. *Phys. Rev. Lett.* **2001**, *87*, 077003.
(3) Imai, M.; Nishida, K.; Kimura, T.; Abe, H. *Appl. Phys. Lett.* **2002**, *80*, 1019.
(4) Imai, M.; Nishida, K.; Kimura, T.; Abe, H. *Phys. C* **2002**, *377*, 96.
(5) Imai, M.; Nishida, K.; Kimura, T.; Kitazawa, H.; Abe, H.; Kito, H.; Yoshii, K. *Phys. C* **2002**, *382*, 361.
(6) Meng, R. L.; Lorenz, B.; Wang, Y. S.; Cmaidalka, J.; Sun, Y. Y.; Xue, Y. Y.; Meen, J. K.; Chu, C. W. *Phys. C* **2002**, *382*, 113.
(7) Lorenz, B.; Lenzi, J.; Cmaidalka, J.; Meng, R. L.; Sun, Y. Y.; Xue, Y. Y.; Chu, C. W. *Phys. C* **2002**, *383*, 191.
(8) Meng, R. L.; Lorenz, B.; Cmaidalka, J.; Wang, Y. S.; Sun, Y. Y.; Lenzi, J.; Meen, J. K.; Xue, Y. Y.; Chu, C. W. *IEEE Trans. Appl. Supercond.* **2003**, *13*, 3042.
(9) Yamanaka, S.; Otsuki, T.; Ide, T.; Fukuoka, H.; Kumashiro, R.; Rachi, T.; Tanigaki, K.; Guo, F.; Kobayashi, K. *Phys. C* **2007**, *451*, 19.
(10) Choi, H. J.; Roundy, D.; Sun, H.; Cohen, M. L.; Louie, S. G. *Nature* **2002**, *418*, 758.
(11) Imai, M.; Sadki, E. H. S.; Abe, H.; Nishida, K.; Kimura, T.; Sato, T.; Hirata, K.; Kitazawa, H. *Phys. Rev. B* **2003**, *68*, 064512.
(12) Shein, I. R.; Medvedeva, N. I.; Ivanovskii, A. L. *J. Phys.: Condens. Matter* **2003**, *15*, L541.
(13) Huang, G. Q.; Chen, L. F.; Liu, M.; Xing, D. Y. *Phys. Rev. B* **2004**, *69*, 064509.
(14) Mazin, I. I.; Papaconstantopoulos, D. A. *Phys. Rev. B* **2004**, *69*, 180512.
(15) Shein, I. R.; Medvedeva, N. I.; Ivanovskii, A. L. *Comput. Mater. Sci.* **2006**, *36*, 203.
(16) Kuroiwa, S.; Nakashima, A.; Miyahara, S.; Furukawa, N.; Akimitsu, J. *J. Phys. Soc. Jpn.* **2007**, *76*, 113705.

Published on Web 07/23/2010

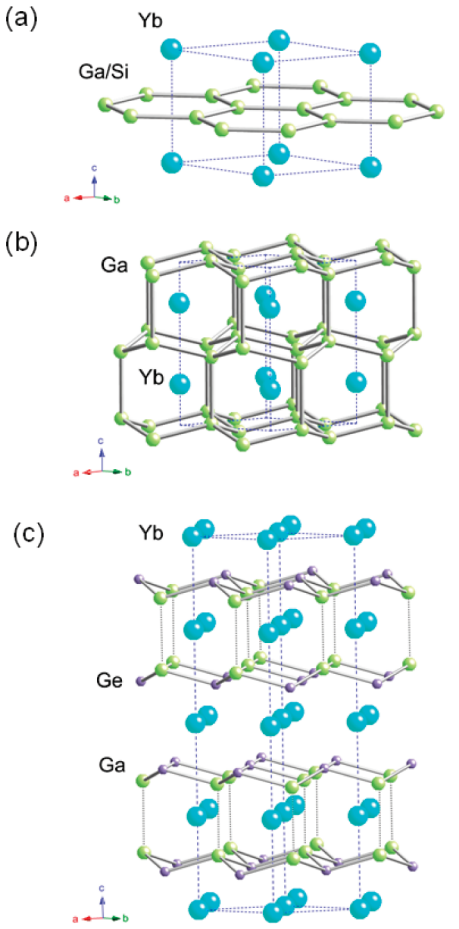

Figure 1. Crystal structures of the $YbGa_xSi_{2-x}$ and related compounds. (a) The AlB_2-type structure for $YbSi_{2-\delta}$ ($\delta = 0.26 - 0.33$) and $YbGa_xSi_{2-x}$ with $x \sim 1.1$, (b) the $CaIn_2$-type structure for $YbGa_2$, and (c) the YPtAs-type structure for YbGaGe.

Recently, a new ternary system $YbGa_{1.1}Si_{0.9}$ has been disclosed as a type-II superconductor with $T_C = 2.4$ K.[17] This compound also has the AlB_2-type structure, in which Ga and Si atoms are distributed two dimensionally to form honeycomb layers. $YbGa_{1.1}Si_{0.9}$ is the first ternary compound characterized in the Yb−Ga−Si system. It should be noted that the binary compound $YbSi_{2-\delta}$ (with $\delta \sim 0.3$) was reported to crystallize in the defected AlB_2-type structure.[18,19] On the other hand, $YbGa_2$ adopts the $CaIn_2$-type structure with the space group $P6_3/mmc$, which is shown in Figure 1b.[20,21] Here, the Ga atoms occupy the 4f site with the atomic position (1/3, 2/3, z) with $z \sim 0.44$. For $z = 1/2$, the structure is identical to the AlB_2-type one. $YbGa_2$ indeed transforms into the UHg_2-type structure above 22 GPa, which is symmetrically the same structure as the AlB_2 type but with a smaller c/a ratio.[22] Then, it is important to address over which chemical composition range the ternary AlB_2-type structure is stabilized for the pseudobinary system $YbGa_xSi_{2-x}$ when x is varied from 0 (ideal composition of $YbSi_{2-\delta}$) to 2 ($YbGa_2$). The superconducting properties of the system are also of interest since neither of the end compounds $YbSi_{2-\delta}$ nor $YbGa_2$ shows superconductivity.[23,24] More generally, the knowledge of the chemical composition dependence of the superconducting properties of $YbGa_xSi_{2-x}$ would provide clues for the understanding of the mechanism behind the occurrence of superconductivity in compounds with the honeycomb layer structure.

Furthermore, superconductivity in Yb compounds is of great interest since the 4f electrons can play some role in superconductivity through the mixed-valency of Yb. It is known that the 4f electrons (f) of Yb hybridize with the conduction electrons (c), resulting in fluctuations of the valence between the divalent and trivalent state. The $c-f$ hybridization, and sometimes the ensuing valence fluctuation, is known to result in the suppression of superconductivity. Thus, absence of superconductivity in the boron−carbide $YbNi_2B_2C$ was attributed to the strong $c-f$ hybridization.[25,26] Examples of Yb-based superconductors reported so far include $YbSb_2$,[27] $Yb_3Rh_4Sn_{13}$,[28,29] $Yb_3Co_{4.3}Sn_{12.7}$,[30] and C_6Yb.[31] In these compounds, Yb has been considered to be in the divalent state (4f,[14] $J = 0$) or very close to it. For instance, band calculation and photoemission spectra showed that Yb is purely divalent in C_6Yb.[32] On the other hand, for $Yb_3Rh_4Sn_{13}$ and $Yb_3Co_{4.3}Sn_{12.7}$, a small contribution of trivalent Yb was observed by X-ray absorption spectroscopy (XAS), resulting in the mean valence $Yb^{2.20+}$ and $Yb^{2.18+}$, respectively.[30,33] For the new $YbGa_{1.1}Si_{0.9}$ system, magnetic susceptibility measurements suggested that Yb may be divalent.[17] This calls for a precise determination of the Yb valence using spectroscopic measurements.

In this paper, we investigate the composition dependence of the phase stability and the superconducting properties of $YbGa_xSi_{2-x}$. In addition, we directly measure the Yb valence by means of bulk-sensitive X-ray spectroscopic

(17) Imai, M.; Sato, A.; Aoyagi, T.; Kimura, T.; Matsushita, Y.; Tsujii, N. *J. Am. Chem. Soc.* **2008**, *130*, 2886.
(18) Palenzona, A.; Manfrinetti, P.; Brutti, S.; Balducci, G. *J. Alloys Compd.* **2003**, *348*, 100.
(19) Iandelli, A.; Palenzona, A.; Olcese, G. L. *J. Less Common Met.* **1979**, *64*, 213.
(20) Iandelli, A. *Z. Anorg. Allg. Chem.* **1964**, *330*, 221.
(21) Palenzona, A.; Cirafici, S. *J. Less Common Met.* **1979**, *63*, 105.
(22) Schwarz, U.; Giedigkeit, R.; Niewa, R.; Schmidt, M.; Schnelle, W.; Cardoso, R.; Hanfland, M.; Hu, Z.; Klementiev, K.; Grin, Y. *Z. Anorg. Allg. Chem.* **2001**, *627*, 2249.
(23) Grytsiv, A; Kaczorowski, D.; Leithe-Jasper, A.; Tran, V. H.; Pikul, A.; Rogl, P; Potel, M.; Noël, H.; Bohn, M.; Velikanova, T. *J. Solid State Chem.* **2002**, *163*, 178.
(24) Sugawara, H.; Motoki, K.; Yamazaki, T.; Ebihara, T.; Kimura, N.; Takashita, M.; Itoh, J.; Toshima, H.; Settai, R.; Ōnuki, Y. *J. Phys. Soc. Jpn.* **1995**, *64*, 3360.
(25) Dhar, S. K.; Nagarajan, R.; Hossain, Z.; Tominez, E.; Godart, C.; Gupta, L. C.; Vijayaraghavan, R. *Solid State Commun.* **1996**, *98*, 985.
(26) Yatskar, A.; Budraa, N. K.; Beyermann, W. P.; Canfield, P. C.; Bud'ko, S. L. *Phys. Rev. B* **1996**, *54*, R3772.
(27) Yamaguchi, Y.; Waki, S.; Mitsugi, K. *J. Phys. Soc. Jpn.* **1987**, *56*, 419.
(28) Remeika, J. P.; Espinosa, G. P.; Cooper, A. S.; Barz, H.; Rowell, J. M.; MacWhan, D. B.; Vandenberg, J. M.; Moncton, D. E.; Fisk, Z.; Woolf, L. D.; Hamaker, H. C.; Maple, M. B.; Shirane, G.; Thomlinson, W. *Solid State Commun.* **1980**, *34*, 923.
(29) Hodeau, J. L.; Chenavas, J.; Marezio, M.; Remeika, J. P. *Solid State Commun.* **1980**, *36*, 839.
(30) Mudryk, Y.; Grytsiv, A.; Rogl, P.; Dusek, C.; Galatanu, A.; Idl, E.; Michor, H.; Bauer, E.; Godart, C.; Kaczorowski, D.; Romaka, L.; Bodak, O. *J. Phys.: Condens. Matter* **2001**, *13*, 7391.
(31) Weller, T. E.; Ellerby, M.; Saxena, S. S.; Smith, R. P.; Skipper, N. T. *Nature Phys.* **2005**, *1*, 39.
(32) Mazin, I. I.; Molodtsov, S. L. *Phys. Rev. B* **2005**, *72*, 172504.
(33) Bordet, P.; Hodeau, J. L.; Wolfers, P.; Krill, G.; Weiss, F.; Marezio, M. *J. Magn. Magn. Mater.* **1987**, *63−64*, 524.

techniques. Finally, we compare the structural and electronic properties of $YbGa_xSi_{2-x}$ with those of superconducting MGa_xSi_{2-x} and nonsuperconducting $YbGa_xGe_{2-x}$.

Experimental Section

Polycrystalline samples of $YbGa_XSi_{2-X}$ were prepared by arc melting and annealing. We use capital X to indicate the loaded (nominal) Ga composition. Later, we will use the small letter x to represent the actual Ga composition determined by the chemical composition. At first, ingots of Yb (3N pure), Ga (6N), and Si (11N) were melted in an arc furnace on a water-cooled Cu hearth under argon atmosphere. A titanium ingot was melted beforehand in order to absorb the residual oxygen in the chamber. A few percent of weight loss was observed after the arc melting. This is attributed to the volatility of Yb, which has a higher vapor pressure compared to the other two elements Ga and Si. The samples were, therefore, melted again with an additional amount of Yb. The samples were turned over and melted several times until reaching a weight loss of less than 1%. We will refer to these samples as as-cast.

The as-cast samples were wrapped with tantalum foils and sealed in evacuated quartz tubes. The tubes were heated in an electric furnace at 1073 K for more than 10 days. The samples were removed from the furnace and allowed to cool down to room temperature. We refer to them as annealed samples.

The structure of the samples was investigated by the powder X-ray diffractometer Rigaku RINT2500 using Cu Kα radiation operating at 40 kV and 300 mA. The lattice parameters were determined from the X-ray diffraction patterns using the RIETAN 2000 program.[34] The chemical compositions were studied by electron probe microanalysis (EPMA) in the wavelength dispersive spectroscopy (WDS) mode. The chemical composition analysis was performed using a prototype field-emission EPMA (remodeled JXA8900R, JEOL) with an accelerating voltage of 15 kV and a beam current of 50 nA. Net elemental intensities were determined with respect to those from crystals of $YbAl_3$, GaP, and Si, which were used for the calibration of Yb, Ga, and Si, respectively. The chemical composition analysis was carried out over ten different points for each sample. The analysis was performed for annealed samples.

Physical property measurements were conducted for single-phase annealed samples. Electrical resistivity was measured from 1.8 to 300 K by the four-probe method with an ac current of 1 mA using a Physical Properties Measurement System (PPMS), Quantum Design Co. Seebeck coefficient was also measured using the PPMS for a bar shaped polycrystalline sample. Magnetic susceptibility was measured from 1.8 to 300 K using a superconducting quantum interference device magnetometer (SQUID), MPMS, Quantum Design Co.

The electronic structure of the Yb ions was studied by means of XAS in the partial fluorescence yield (PFY) mode. The measurements were carried out at the beamline BL15XU at SPring-8, Japan. Details about the measurement method were published elsewhere.[35−38] PFY−XAS spectra were obtained by measuring the intensity of the peak of the $L\alpha_1$ fluorescence line while scanning the incident photon energy across the Yb L_{III}-edge. The PFY−XAS spectra are free from the core-hole lifetime; hence, they benefit from a higher energy resolution than the conventional XAS spectra.[39,40] Accordingly, the mean Yb valence was first estimated by fitting the PFY−XAS spectra. In order to further increase the accuracy of our analysis, we also used resonant inelastic X-ray scattering (RIXS) spectroscopy, a powerful tool to derive the absolute value of the valence.[35,36] Details about the RIXS procedure are given in the Supporting Information. Both PFY−XAS and RIXS yielded consistent values of the valence. For the measurement of the temperature dependence, an Iwatani CRT-M310-OP cryostat was used to cool down the samples from room temperature to about 18 K.

Results and Discussion

A. Phase Relation of the AlB_2-Type Phase in the $YbGa_xSi_{2-x}$ System. Powder X-ray diffraction (XRD) patterns for the as-cast samples of $YbGa_XSi_{2-X}$ with the nominal composition $X = 1.0-1.5$ showed the existence of the phase with the AlB_2-type structure, as well as other phases such as $YbSi_{2-\delta}$, YbSi, etc. Annealing up to 1073 K resulted in the formation of single-phase samples with the AlB_2-type structure for a wide composition range. This indicates that the AlB_2-type $YbGa_XSi_{2-X}$ compounds melt incongruently, which limits the possibility to obtain large single crystalline samples. Trials to grow single crystals using gallium and tin flux were unsuccessful. Then, we used polycrystalline samples for the physical property measurements.

Figure 2 shows the powder X-ray diffraction (XRD) pattern of the annealed $YbGa_XSi_{2-X}$ with $X = 1.0-1.5$. The results for $X = 1.15-1.4$ show almost pure phase with the AlB_2-type structure, with only tiny peaks assigned to Yb_2O_3. The intensity of the peak due to Yb_2O_3 at $2\theta = 29.6°$ is approximately 1% with respect to that of the (101) peak for the AlB_2-type phase. For $X \geq 1.5$, additional peaks appear which are indexed as $YbGa_2$ or its alloy with Si. For $X \leq 1.15$, diffraction peaks from an unknown phase develop with decreasing X. The unknown phase is likely to have a tetragonal unit cell, suggesting the existence of a new Yb−Ga−Si ternary phase.

All the samples except $X = 1.5$ were stable in air and water. The powder X-ray diffraction pattern taken after being kept in air for several days showed no change from the initial pattern. For $X = 1.5$, the sample ingot was found to be decomposed into powder within a few days in air. This is probably due to the decomposition of the $YbGa_2$ phase involved in the $X = 1.5$ sample.

In Table 1, we list the chemical composition of the main phase determined by EPMA/WDS. Here, the composition is expressed in the formula of $Yb_{1-\delta}(Ga_xSi_{2-x})$. The small values of δ indicate that the atomic ratios Yb/(Ga + Si) are almost 1:2. We, therefore, neglect the deficiency δ

(34) Izumi, F.; Ikeda, T. *Mater. Sci. Forum* **2000**, *321−324*, 198.
(35) Yamaoka, H.; Tsujii, N.; Yamamoto, K.; Oohashi, H.; Vlaicu, A. M.; Kunitani, K.; Uotani, K.; Horiguchi, D.; Tochio, T.; Ito, Y.; Shin, S. *Phys. Rev. B* **2007**, *76*, 075130.
(36) Yamamoto, K.; Yamaoka, H.; Tsujii, N.; Vlaicu, A. M.; Oohashi, H.; Sakakura, S.; Tochio, T.; Ito, Y.; Chainani, A.; Shin, S. *J. Phys. Soc. Jpn.* **2007**, *76*, 124705.
(37) Yamaoka, H.; Tsujii, N.; Yamamoto, K.; Vlaicu, A. M.; Oohashi, H.; Yoshikawa, H.; Tochio, T.; Ito, Y.; Chainani, A.; Shin, S. *Phys. Rev. B* **2008**, *78*, 045127.
(38) Yamaoka, H.; Jarrige, I.; Tsujii, N.; Hiraoka, N.; Ishii, H.; Tsuei, K. D. *Phys. Rev. B* **2009**, *80*, 035120.
(39) Hämäläinen, K.; Siddons, D. P.; Hastings, J. B.; Berman, L. E. *Phys. Rev. Lett.* **1991**, *67*, 2850.
(40) Åberg, T.; Tulkki, T. In *Atomic and Inner-Shell Physics*; Crasemann, Ed.; Plenum: New York, 1985; p.145.

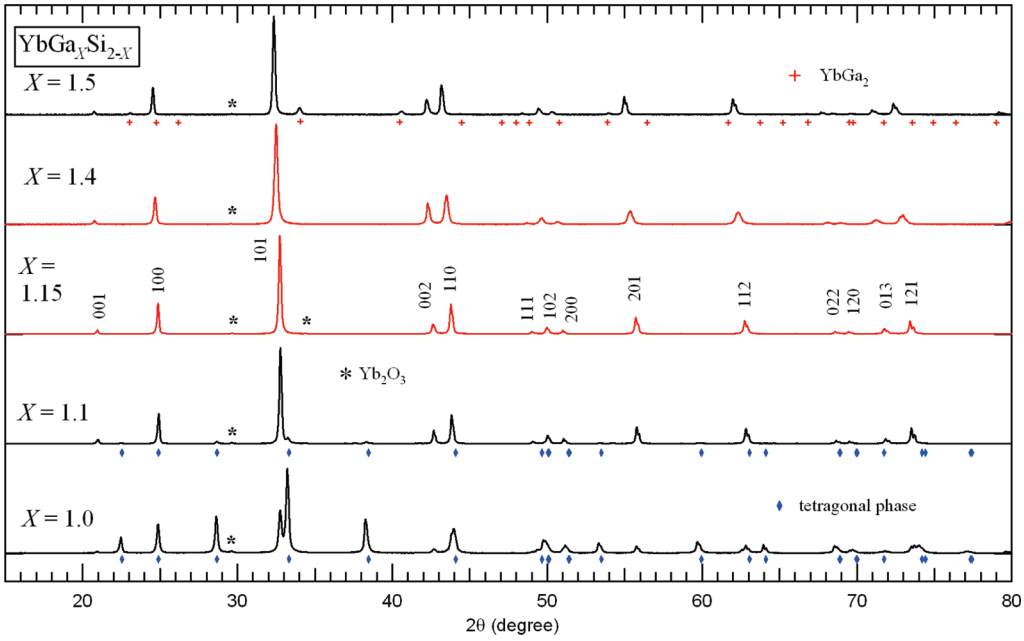

Figure 2. Powder XRD patterns of annealed $YbGa_XSi_{2-X}$ samples. The composition X indicates nominal one. The asterisks are diffraction peaks from Yb_2O_3.

Table 1. Chemical Composition of the Annealed Samples Determined from EPMA[a]

	atomic %				
X (nominal)	Yb	Ga	Si	chemical formula	x (EPMA)
1.1	32.83 (0.11)	37.76 (0.19)	29.39 (0.19)	$Yb_{0.985(3)}Ga_{1.124(5)}Si_{0.876(5)}$	1.12 (1)
1.15	32.80 (0.11)	38.62 (0.13)	28.57 (0.13)	$Yb_{0.984(4)}Ga_{1.149(4)}Si_{0.851(4)}$	1.15 (1)
1.2	32.74 (0.21)	40.24 (0.41)	27.02 (0.46)	$Yb_{0.982(6)}Ga_{1.197(13)}Si_{0.803(13)}$	1.20 (2)
1.25	33.08 (0.13)	42.14 (0.17)	24.77 (0.15)	$Yb_{0.993(4)}Ga_{1.260(4)}Si_{0.740(4)}$	1.26 (1)
1.3	32.67 (0.18)	43.96 (0.27)	23.34 (0.30)	$Yb_{0.980(5)}Ga_{1.306(8)}Si_{0.694(8)}$	1.31 (1)
1.4	32.93 (0.10)	47.28 (0.45)	19.77 (0.45)	$Yb_{0.988(3)}Ga_{1.410(13)}Si_{0.590(13)}$	1.41 (1)
1.5	32.60 (0.11)	50.14 (1.03)	17.26 (0.98)	$Yb_{0.978(3)}Ga_{1.488(29)}Si_{0.512(29)}$	1.49 (3)

[a] The chemical formulas are expressed to meet the formula $Yb_{1-d}(Ga_xSi_{2-x})$.

for the Yb site and, hereafter, describe the chemical composition just as $YbGa_xSi_{2-x}$ using the small letter x referring to the Ga composition determined from EPMA. For the sample with the nominal composition $X = 1.1$, the XRD pattern can be explained by the coexistence of an AlB_2-type phase and a tetragonal phase. The EPMA result on this sample revealed two distinct regions corresponding to the respective phases with chemical compositions of $x = 1.12$ and $x \sim 0.8$. Then, we can conclude that the former value ($x = 1.12$) is the lower limit of x for the AlB_2-type phase. This agrees well with the previous result.[17] The composition $x \sim 0.8$ is attributed to that of the new tetragonal phase. Details for this phase will be published elsewhere. The presence of the new $YbGa_xSi_{2-x}$ phase with $x \sim 0.8$ indicates that the AlB_2-type $YbGa_xSi_{2-x}$ phase is not neighbored by $YbSi_{2-\delta}$ though it crystallizes in the defected AlB_2-type structure.

For the nominal composition $X = 1.5$, where the XRD pattern showed the coexistence of the AlB_2-type structure and $YbGa_2$, the chemical composition of the majority phase was found to be $x = 1.49(3)$ by EPMA, which should be the upper limit of Ga concentration for the AlB_2-type phase. We were unable to analyze the chemical composition of the minority phase, $YbGa_2$ or its alloy, since it decomposed during the process of surface polishing. We then conclude that the AlB_2-type phase is stabilized in the composition range of $1.12(1) \leq x \leq 1.49(3)$.

In Figure 3, the lattice parameters a and c, the unit cell volume V, and the ratio c/a are shown as a function of Ga concentration x. Both a and c increase linearly with x. This causes a monotonic increase of V, whereas the ratio c/a remains between 1.02 and 1.03.

B. Transport Properties. In Figure 4, the temperature dependence of the electrical resistivity, $\rho(T)$, is shown. All samples show metallic behavior. The absolute value of resistivity at room temperature, ρ(300 K), increases from 160 $\mu\Omega$cm for $x = 1.15$ to 380 $\mu\Omega$cm for $x = 1.41$. Although the absolute value of the resistivity can be ambiguous because of both the error on the estimation of sample dimensions and the random scatterings of electrons at the grain boundaries, the increase in ρ(300 K) with x was observed reproducibly in our experiments; thereby, we believe it to be intrinsic. One possible explanation can be the increase of the disorder in the Ga/Si layer with x. This is, however, ruled out since the previous X-ray diffraction experiment using a single crystalline $YbGa_{1.13}Si_{0.87}$ suggested that Ga and Si atoms occupy the honeycomb layer sites randomly, and no indication of atomic order or

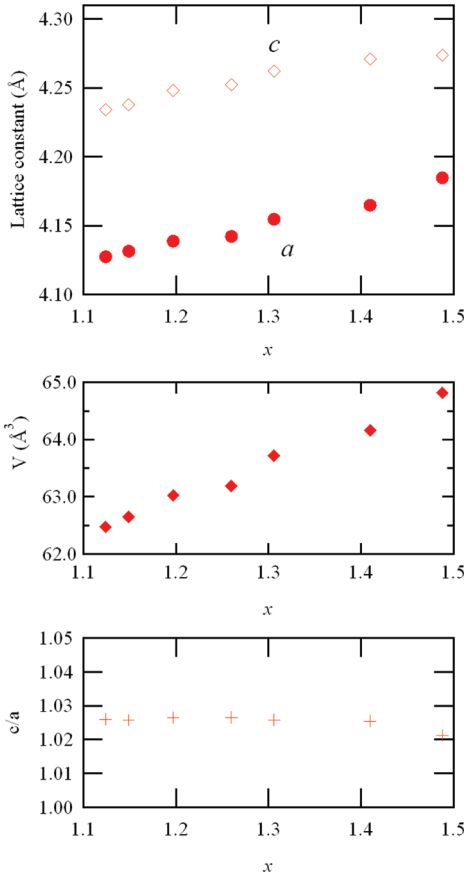

Figure 3. Lattice constants a and c, lattice volume V, and the ratio c/a for $YbGa_xSi_{2-x}$. x was determined by EPMA. Errors are within the size of the markers.

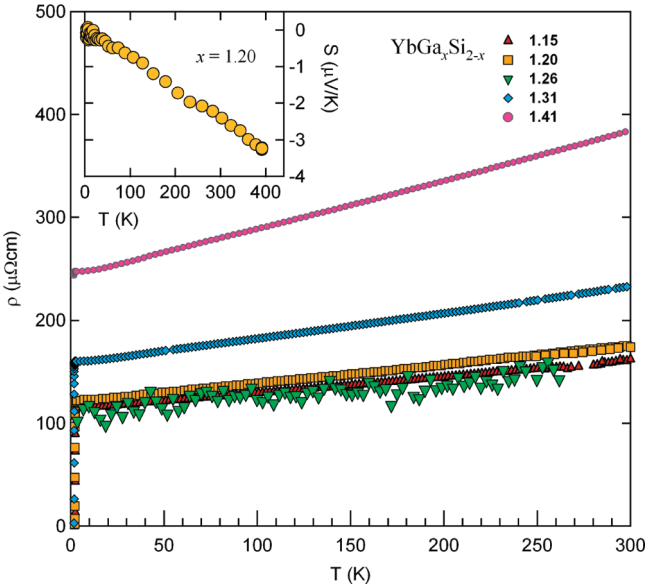

Figure 4. Temperature dependence of electrical resistivity $\rho(T)$ for $YbGa_xSi_{2-x}$ measured on the heating process. Inset: Temperature dependence of the Seebeck coefficient S(T) for $x = 1.20$.

superstructure was obtained.[17] Another possible origin is the decrease of carrier concentration as x is increased. Dominant carriers of the present system are likely to be electrons, since the Seebeck coefficient $S(T)$ for $x = 1.20$ is negative throughout the measured T range, as is shown

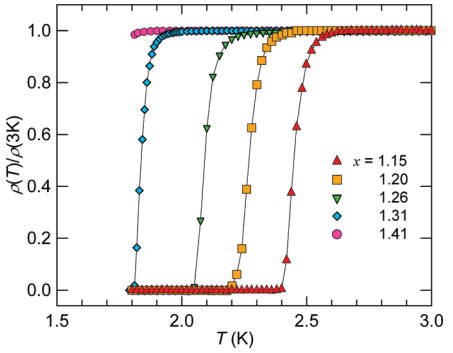

Figure 5. Electrical resistivity at low temperatures normalized by the values at 3 K for $YbGa_xSi_{2-x}$.

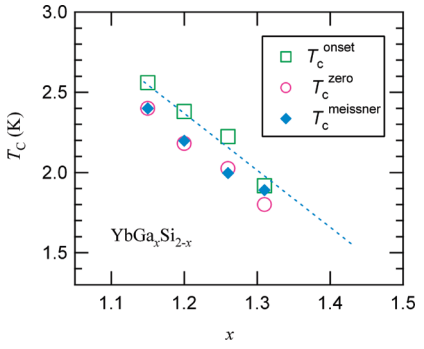

Figure 6. Ga-concentration dependence of the superconducting transition temperature T_C for $YbGa_xSi_{2-x}$. The broken line is a guide for the eye.

in the inset of Figure 4. Negative $S(T)$ was also reported for CaAlSi, SrAlSi, and SrGaSi,[7,8] and the Hall coefficient measurement confirmed that electrons are the major carriers for CaAlSi.[11] Now, the total number of valence electrons in $YbGa_xSi_{2-x}$ is expected to decrease when Si is replaced by Ga, which can lead to the decrease in the carrier electron concentration.

The low-temperature resistivity data normalized by their value at $T = 3$ K are shown in Figure 5. There is a sharp drop in $\rho(T)$ of $x = 1.15$ at $T = 2.5$ K, indicating the onset of superconducting transition. Zero resistivity is observed at $T = 2.4$ K for $x = 1.15$. Superconducting transition is also observed for $x = 1.20$, 1.26, and 1.31, with the critical temperature T_C decreasing with increasing x. For $x = 1.41$, one can see that the resistivity just starts to decrease at 1.8 K, suggesting a further shift of T_C toward low temperature.

We define the onset temperature of superconductivity, T_C^{onset}, to be the temperature where the resistivity has decreased 5% compared with ρ(3K). T_C^{onset} is plotted as a function of x in Figure 6, along with the temperature at which the resistivity becomes zero, T_C^{zero}. For $x = 1.41$, we can expect T_C^{onset} around 1.5−1.6 K. $T_C^{zero} = 2.4$ K for $x = 1.15$ is in good agreement with the previous report.[17]

C. Magnetic Properties. Figure 7 shows the volume magnetization divided by the applied field, M/H, of $YbGa_xSi_{2-x}$ below 3K measured under a field of $H = 10$ Oe. M/H was measured in zero-field-cooled (ZFC) and field-cooled (FC) mode. M/H in both ZFC and FC shows

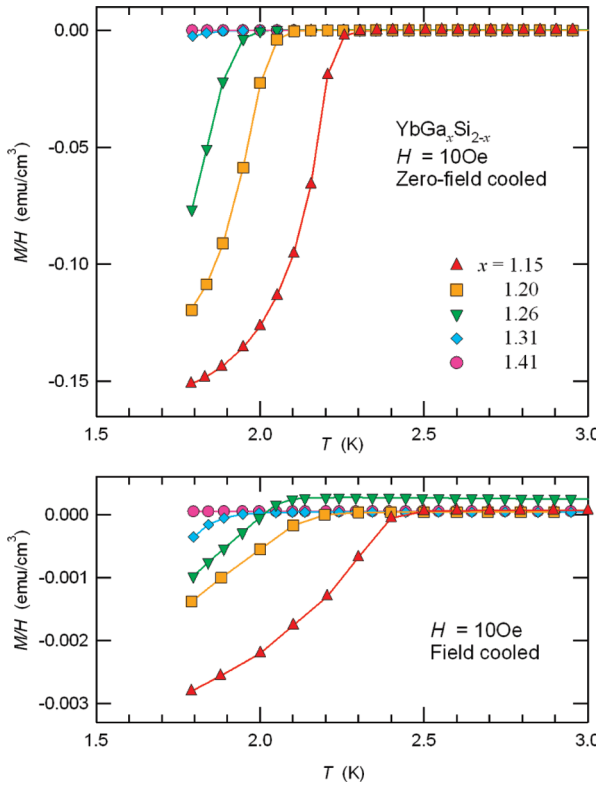

Figure 7. Magnetization divided by the applied field, M/H, at low temperature as a function of the temperature measured under low magnetic fields of $H = 10$ Oe.

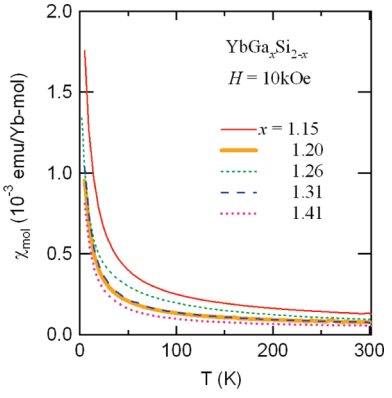

Figure 8. Temperature dependence of the magnetic susceptibility for $YbGa_xSi_{2-x}$ measured at $H = 10$ kOe.

negative values at low temperatures, corresponding to the Meissner effect due to the superconducting transition. We define $T_C^{Meissner}$, shown in Figure 6, as the temperature below which M/H in the FC mode becomes negative. $T_C^{Meissner}$ agrees well with T_C^{zero} obtained from resistivity.

Assuming a sphere-shaped superconducting material, the demagnetization factor is $\alpha = 1/3$ and the magnetic susceptibility for the ZFC data of $x = 1.15$ at 1.8 K is estimated by $\chi_v = M/H \times (1 - \alpha) = -0.10$ emu/cm^3. This value is close to the perfect diamagnetism, $-1/4\pi \sim -0.080$ emu/cm^3. This indicates that the superconductivity observed for $YbGa_xSi_{2-x}$ is a bulk effect.

In Figure 8, we show the temperature dependence of the magnetic susceptibility, $\chi(T)$, measured under the constant field $H = 10$ kOe. For all measured samples, the

Table 2. Magnetic Parameters Obtained from the Curie-Weiss Fittings to the Magnetic Susceptibility Data for $YbGa_xSi_{2-x}$[a]

x	C (emu K/mol)	θ (K)	Yb^{3+} concentration
1.15	0.0234 (3)	−20 (1)	0.0091 (12)
1.20	0.0093 (4)	−8 (2)	0.0037 (2)
1.26	0.0219 (1)	−31 (1)	0.0085 (1)
1.31	0.0098 (2)	−7 (1)	0.0038 (1)
1.41	0.0064 (1)	−0.8 (4)	0.0025 (1)

[a] Yb^{3+} concentration was estimated from the Curie constant.

susceptibility increases rapidly with decreasing T, which is a typical behavior of paramagnetic ions with local magnetic moments. We analyzed the data above 50 K by a Curie−Weiss law, $\chi(T) = C/(T - \theta) + \chi_0$, where C, θ, and χ_0 are the Curie constant, Weiss temperature, and the temperature-independent term, respectively. The Curie constant is expressed using the number of magnetic ions N, the Landé g factor g_J, the total angular momentum J, Bohr magneton μ_B, and the Boltzmann constant k_B, as $C = Ng_J^2J(J+1)\mu_B^2/3k_B$. This equation allows us to estimate the number of Yb^{3+} ions, since Yb^{2+} is nonmagnetic ($J = 0$) and only Yb^{3+} possesses magnetic moment, $J = 7/2$ with $g_J = 8/7$. When one formula unit involves one Yb^{3+} ion, the Curie constant should be $C = 2.57$ emu K/mol. Here, the unit of mol indicates the formula-unit mol. The results of the fits of C and θ are listed in Table 2. The yielded ratio of Yb^{3+} is found to be less than 1% for all x values. This suggests that most of the Yb ions in the $YbGa_xSi_{2-x}$ phase are in the divalent ($4f^{14}$, $J = 0$) state.

However, it should be noted that the analysis from magnetic susceptibility only yields the amount of stable Yb^{3+} ions that obey Curie−Weiss laws. In metallic compounds, Yb ions can be in a valence-fluctuating state $Yb^{2+\leftrightarrow 3+}$ and show significant deviation from the Curie−Weiss type susceptibility, behaving like a nonmagnetic metal at low temperature.[41−46] For such valence fluctuating compounds, Curie−Weiss behavior is only observed at elevated temperatures.[41−46] One remarkable example is $YbCu_{5-x}Al_x$.[47] X-ray absorption revealed the successive change in the Yb valence with decreasing x: for $1.5 \leq x$, a stable Yb^{3+} state is observed, while Yb tends to show mixed valence behavior for $x = 0.5-1.0$; eventually, $x = 0$ shows $Yb^{2.4+}$, close to the nonmagnetic divalent state.[36,38,47] Concomitantly, magnetic susceptibility $\chi(T)$ of $YbCu_{5-x}Al_x$ also shows successive change with x. Curie−Weiss behavior with the full Yb^{3+} moment is observed for $1.5 \leq x$.[47] With decreasing x, $\chi(T)$ decreases and tends to show a maximum at T_{max}, which shifts to higher temperatures from 200 K ($x = 0.8$) to 600 K

(41) Lawrence, J. M.; Riseborough, P. S.; Parks, R. D. *Rep. Prog. Phys.* **1981**, *44*, 1.
(42) Klaasse, J. C. P.; de Boer, F. R.; de Châtel, P. F. *Phys. B* **1981**, *106*, 178.
(43) Danan, J.; de Novion, C.; Lallement, R. *Solid State Commun.* **1969**, *7*, 1103.
(44) Shaheen, S. A.; Schilling, J. S.; Liu, S. H.; McMasters, O. D. *Phys. Rev. B* **1983**, *27*, 4325.
(45) Bauer, E. *Adv. Phys.* **1991**, *40*, 417.
(46) Kishimoto, Y.; Kawasaki, Y.; Ohno, T. *Phys. Lett. A* **2003**, *317*, 308.
(47) Bauer, E.; Hauer, R.; Keller, L.; Fischer, P.; Trovarelli, O.; Sereni, J. G.; Rieger, J. J.; Stewart, G. R. *Phys. Rev. B* **1997**, *56*, 711.

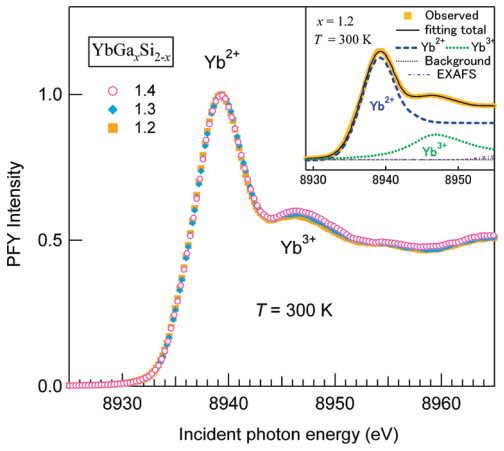

Figure 9. X-ray absorption spectra with the partial fluorescence yield mode (PFY−XAS) measured at the L_{III} edge of Yb as a function of incident energy for $YbGa_xSi_{2-x}$. The data are normalized by the intensity at the maxima. The inset explains the curve fitting procedure. The observed spectrum is expressed as the sum of the background, the XAS of L_{III} edge of Yb^{2+} and Yb^{3+}, and the extended X-ray absorption fine structure (EXAFS).

($x = 0.5$) with decreasing x.[48,49] Curie−Weiss behavior is seen above T_{max}, whereas $\chi(T)$ below T_{max} shows a nearly nonmagnetic behavior. For $x = 0$ in which a mixed valent state of $Yb^{2.4+}$ is observed, normal Curie−Weiss behavior is only expected at $T > 1000$ K. These examples point to the fact that Curie−Weiss fitting does not yield an exact valence when strong valence fluctuation takes place. This stresses the need to resort to X-ray spectroscopic measurements to evaluate the true valence of Yb ions in valence-fluctuating compounds. The results are shown in the following section.

D. X-ray Spectroscopy Study. X-ray spectroscopic measurements enable one to resolve the mixed valent state ($Yb^{2+\leftrightarrow 3+}$) into two spectroscopic components corresponding, respectively, to the integer-states Yb^{2+} and Yb^{3+} even in the case of fluctuating valence, as has been shown for many materials.[35−38,50,51] We employed PFY−XAS which, in the hard X-ray regime, provides truly bulk-sensitive information about the electronic structure. Thus, we can neglect the surface effect, which sometimes is a problem for X-ray photoelectron spectroscopy.[35,51] In Figure 9, the PFY−XAS spectra measured at the Yb L_{III} edge are shown. Details about the fitting procedure, illustrated in the inset of Figure 9, can be found elsewhere.[35−38] We measured three annealed samples of $YbGa_xSi_{2-x}$ with x and determined them to be 1.19, 1.28, and 1.42 by EPMA. Hereafter, we refer to these samples as $x = 1.2$, 1.3, and 1.4, respectively. The spectra in Figure 9 are normalized to the top peak near 8940 eV, which is assigned to Yb^{2+}. On the other hand, the second peak around 8947 eV corresponds to the Yb^{3+} contribution. The Yb valences estimated through fitting are 2.310+, 2.312+, and 2.328+ for $x = 1.2$, 1.3, and 1.4, respectively. We estimate the error on these values to be approximately ±0.01. The value of the valence shows a very slight increase (∼ 1%) when x increases from 1.2 to 1.4. It is unclear whether this x dependence of the valence is intrinsic or whether it could be related to a contamination of Yb_2O_3 or another minor phase such as YbSi.[52] We measured the PFY−XAS spectrum for the three compounds at 18 K too, but no temperature dependence was observed with respect to the spectrum at 300 K. This indicates that the valence remains unchanged down to 18 K.

With RIXS, one has the possibility to selectively enhance each of the Yb^{2+} and Yb^{3+} features; the valence can, therefore, be derived with greater accuracy than PFY−XAS. As shown in the Supporting Information, the value of the valence derived by RIXS agrees well with that estimated by PFY−XAS. We can, therefore, conclude that the mean valence of Yb is ∼2.3+, indicating 30% of Yb is in the trivalent state. This is at odds with the estimation based on the magnetic susceptibility of less than 1% of Yb^{3+}. This means that Yb ions are in the valence fluctuating state, as has been explained in the previous section. When a strong valence fluctuation is realized, Curie−Weiss behavior is only expected at temperatures above the characteristic temperature related to the strength of the c−f hybridization. For the present system, the characteristic temperature should be much higher than room temperature, since no valence change has been observed in PFY−XAS between 18 and 300 K. We stress that the combination of XAS and magnetic susceptibility has given the conclusive information about the valence of Yb. While X-ray spectroscopy is highly powerful to determine the mean valence, it is difficult to distinguish the homogeneous valence fluctuation ($Yb^{2.3+}$) and the heterogeneously distributed mixed valence ($7Yb^{2+} + 3Yb^{3+}$). Examples of the latter case are $Yb_9Zn_4Bi_9$ and $Yb_7Co_4InGe_{12}$.[53,54] Since the magnetic susceptibility indicated that the stable Yb^{3+} ions are almost absent for the present case, we can rule out the heterogeneous mixed valence. Therefore, the valence $Yb^{2.3+}$ determined from the PFY−XAS and RIXS indicates that Yb ions are in the valence fluctuating state ($Yb^{2+\leftrightarrow 3+}$). The small Curie constant corresponding to less than 1% of Yb^{3+} is attributed to tiny amount of impurities, such as Yb_2O_3. Indeed, specific heat results, shown in the Supporting Information section, demonstrate that about 0.4% of Yb exists as Yb_2O_3.

It has been shown that $Yb_3Co_{4.3}Sn_{12.7}$ is a superconductor with $T_C = 3.4$ K and has a mean valence of $Yb^{2.18+}$, while isostructural $Yb_3Co_4Ge_{13}$ does not show superconductivity and has a mean valence of $Yb^{2.66+}$.[30]

(48) Yoshimura, K.; Tsujii, N.; He, J.; Kawabata, T.; Michor, H.; Kreiner, K.; Hilscher, G.; Miyano, T.; Kato, M.; Kosuge, K. *Mater. Struct. Chem., Biol., Phys. Technol.* **1998**, *5*, 245.
(49) He, J.; Ling, G.; Ye, Z. *J. Alloys Compd.* **2001**, *325*, 54.
(50) Dallera, C.; Grioni, M.; Shukla, A.; Vankó, G.; Sarrao, J. L.; Rueff, J. P.; Cox, D. L. *Phys. Rev. Lett.* **2002**, *88*, 196403.
(51) Moreschini, L.; Dallera, C.; Joyce, J. J.; Sarrao, J. L.; Bauer, E. D.; Fritsch, V.; Bobev, S.; Carpene, E.; Huotari, S.; Vankó, G.; Monaco, G.; Lacovig, P.; Panaccione, G.; Fondacaro, A.; Paolicelli, G.; Torelli, P.; Grioni, M. *Phys. Rev. B* **2007**, *75*, 035113.
(52) Engkagul, C.; Selim, R.; Mihalisin, T.; Schlottmann, P. *Phys. Rev. B* **1987**, *35*, 3686.
(53) Chondroudi, M.; Balasubramanian, M.; Welp, U.; Kwok, W. K.; Kanatzidis, M. G. *Chem. Mater.* **2007**, *19*, 4769.
(54) Kim, S. J.; Salvador, J.; Bilc, D.; Mahanti, S. D.; Kanatzidis, M. G. *J. Am. Chem. Soc.* **2001**, *123*, 12704.

In $Yb_3Rh_4Sn_{13}$,[33] for which two phases are known to exist, superconductivity was observed in the phase I with $T_C = 8$ K,[28] whereas no superconductivity was observed for the phase II down to 0.1 K.[33] By XAS, a nearly divalent state ($Yb^{2.20+}$) was found in the phase I, while a higher valence was observed for the phase II ($Yb^{2.50+}$).[33] These examples suggest that superconductivity appears only when the valence of the Yb ions is closer to divalence than trivalence, thus where the magnetic interactions play a minor role. This trend seems not to be restricted to Yb compounds, since the AlB_2-type EuGaSi does not show superconductivity while the Eu ions are in the divalent state with the electronic configuration (4f),[7] hence having the magnetic moment $J = 7/2$.[55]

E. Electronic State of $YbGa_xSi_{2-x}$. The relationship between electronic state and the crystal structure is an important issue.[56] To form a honeycomb layer sheet, three σ and one π bonds are necessary, which accommodate four valence electrons per site. Since Ga and Si provide three and four valence electrons, respectively, the total valence electron number of $YbGa_xSi_{2-x}$ is written as $(10.3 - x)$, with the effect of mixed valence $Yb^{2.3+}$ taken into consideration. The formula is then schematically written as $Yb^{2.3+}Ga_x{}^{1-}Si_{1-x}{}^{0+}\cdot(2.3 - x)e^-$. This leads to eight valence electrons being used to build up the Ga−Si layer, and there are $(2.3 - x)$ extra electrons that do not belong to the layer. Given the composition range of $1.12 \leq x \leq 1.49$, this extra electron number is 1.18−0.81 per formula unit, linearly decreasing with x. These electrons are considered to be responsible for the metallic conductivity. This is consistent with the negative Seebeck coefficient observed for $x = 1.20$, and the increase of the room temperature resistivity ρ(300 K) with x also agrees with the decrease in the electron number. However, band calculations for the AlB_2-type ternary silicides such as CaAlSi and EuGaSi revealed a covalency between the d orbitals of the alkali-earth atoms or Eu and the π orbital of the honeycomb layer.[12−16,55,57] Thus, a clear separation of electrons into bonding and conduction ones is unrealistic. Nevertheless, it is worth mentioning that band calculation for Eu(II)GaSi suggests that there is a pseudogap in the density of states at the energy of about 1 eV lower than the Fermi level, which corresponds to eight valence electrons per formula unit.[55,57] This indicates that such an electron counting or the Zintl−Klemm formalism is valid at least partially to explain the relation of the valence electron number and the crystal structure for these AlB_2-type ternary silicides.

The covalency between the d orbital of the intercalant and the p orbital of the honeycomb layer indicates that some part of the extra $(2.3 - x)$ electrons exist on the Yb sites, which may raise a question about the electronic charge of $Yb^{2.3+}$. However, it should be stressed that the term "valence" for lanthanoids is usually used to distinguish the 4*f* occupation number rather than the actual electronic charge; Yb^{2+} and Yb^{3+} mean $(4f)^{14}$ and $(4f)^{13}$ electronic states, respectively. This 4f occupation number is essential for most of the properties in solids, including magnetic properties, X-ray absorption spectra, lattice volume, etc. Therefore, we still define the valence of Yb to be the value determined by the X-ray spectroscopy.

Table 3. Lattice Parameters and T_C^{onset} of AlB_2-Type Gallium Silicides[a]

	a (Å)	c (Å)	c/a	V (Å^3)	T_C^{onset} (K)
CaGaSi	4.1200 (8)	4.4401 (1)	1.078	65.27	4.5
SrGaSi	4.1875 (4)	4.7447 (4)	1.133	72.05	5.2
BaGaSi	4.2587 (4)	5.1039 (9)	1.198	80.17	4.1
$YbGa_{1.15}Si_{0.85}$	4.1315 (2)	4.2378 (2)	1.026	62.65	2.6

[a] Data for CaGaSi, SrGaSi, and BaGaSi are taken from refs 4 and 5.

The composition variation of T_C in $YbGa_xSi_{2-x}$ indicates a monotonic suppression of superconductivity when the Ga concentration is increased. This agrees with the behaviors of all the MGa_xSi_{2-x} (M = Ca, Sr, Ba) systems, which show a maximum in T_C around $x \sim 1$, above which T_C decreases monotonically.[6,8] The slope of the decrease of T_C as a function of x has been estimated for MGa_xSi_{2-x} with $x > 1$ to be approximately $\Delta T_C/\Delta x = 5$ to 6 K.[6,8] We here estimate the ratio for $YbGa_xSi_{2-x}$ to be $\Delta T_C/\Delta x \sim 5.5$ K, in good agreement with the values for the MGa_xSi_{2-x} systems. The origin of the composition dependence of T_C in $YbGa_xSi_{2-x}$ is, therefore, likely the same as for MGa_xSi_{2-x}.

The variation of the lattice constants was suggested to affect T_C in the AlB_2-type silicides.[9] Common for both $YbGa_xSi_{2-x}$ and MGa_xSi_{2-x} is the monotonic increase in the lattice parameter a with x.[6,8] The expansion of a should weaken the in-plane bond strength. At the same time, the increase of the Ga concentration leads to the increase in the mass of the honeycomb layer. Both of them can cause a decrease in the phonon frequencies, resulting in the suppression of superconductivity. This effect appears to explain the monotonic decrease of T_C for $1.0 < x$ in the MGa_xSi_{2-x} systems but does not appear for the maximum of T_C around $x = 1$ observed for all the MGa_xSi_{2-x} systems.[6,8] The maximum around $x = 1$ may imply that the optimum carrier concentration meets around this stoichiometory. Interestingly, superconductivity was reported to occur in the AlB_2-type $LaGa_2$,[58] which has nine valence electrons like in MAlSi and MGaSi, whereas superconductivity is not reported for the isostructural MGa_2 which has eight valence electrons.[8] Studies of $LaGa_xSi_{2-x}$ may give a hint for the origin of the composition dependence of T_C in the ternary silicides.

F. Comparison with Related Systems. In this section, $YbGa_xSi_{2-x}$ is compared with MGaSi systems and with YbGaGe. Table 3 shows the lattice parameters a and c, the ratio c/a, the lattice volume V, and the onset T_C for the MGaSi compounds taken from the literature[5] and $YbGa_{1.15}Si_{0.85}$. All a, c, and V increase with the mass of the M atom for MGaSi, while c and V are smaller for $YbGa_{1.15}Si_{0.85}$ than CaGaSi. The ionic radii of Yb^{2+} and Yb^{3+} are 1.13 and 0.86 Å, respectively, we can,

(55) You, T.-S.; Grin, Y.; Miller, G. J. *Inorg. Chem.* **2007**, *46*, 8801.
(56) Kauzlarich, S. M., Ed. *Chemistry, Structure, and Bonding of Zintl Pases and Ions*; VCH Publishers: New York, 1996.
(57) You, T.-S.; Zhao, J.-T.; Pöttgen, R.; Schnell, W.; Burkhardt, U.; Grin, Y.; Miller, G. J. *J. Solid State Chem.* **2009**, *182*, 2430.
(58) Fujimaki, Y.; Satoh, K.; Onuki, Y. *J. Phys. Soc. Jpn.* **1992**, *61*, 395.

therefore, roughly estimate the effective ionic radius of $Yb^{2.3+}$ to be 1.05 Å. The ionic radii for M = Ca^{2+}, Sr^{2+}, and Ba^{2+} are 1.06, 1.27, and 1.43 Å, respectively. The small c and V of $YbGa_{1.15}Si_{0.85}$ are, thus, understood to arise from the small ionic radius of $Yb^{2.3+}$.

Now, we discuss the material dependence of T_C. Let us first mention that recent electron diffraction experiments on CaGaSi have revealed the existence of a superstructure along the c axis with a possible corrugation within the honeycomb layer.[59] Such a structural peculiarity is considered to affect the superconducting properties significantly, as observed in CaAlSi.[60−63] To discuss the trend of T_C, we, therefore, focus on the other three compounds, SrGaSi, BaGaSi, and $YbGa_{1.15}Si_{0.85}$, where no structural modification from the AlB_2 structure has been observed. While T_C of the three compounds does not appear to be linked to the lattice constants or lattice volume, it appears to decrease in accordance with the increase in the M atomic mass. In the BCS theory, T_C is roughly dependent on $m^{-1/2}$, where m is the mass of the atom involved in the phonon mode mediating the formation of Cooper pairs. Using T_C = 5.2 K for SrGaSi and the ratio $(m_{Ba}/m_{Sr})^{-1/2} \sim 0.8$ and $(m_{Yb}/m_{Sr})^{-1/2} \sim 0.7$, the relation yields T_C for BaGaSi and a hypothetical YbGaSi to be 4.2 and 3.6 K, respectively. These values seem to be in reasonable agreement with the experimental ones, as the linear extrapolation toward x = 1.0 suggests T_C for hypothetical YbGaSi is about 3.3 K. Furthermore, band calculations showed that the d orbitals of the M atoms play an essential role for the superconductivity. It is then probable that the phonon mode involving the M atoms couples with the on-site d orbitals to cause superconductivity in the MGaSi systems. A similar mechanism has been proposed for the honeycomb layer superconductor CaC_6. The calculation for CaC_6 suggested that it is the vibration of the Ca atoms, coupling with the interlayer band, that is responsible for the occurrence of superconductivity.[64] The Ca isotope effect in CaC_6 confirmed that the phonon mode of the Ca ions plays an essential role for the superconductivity.[65]

For CaAlSi, on the other hand, the out-of-plane phonon mode within the honeycomb layer has been suggested to be relevant for superconductivity,[13,14] and the softening of the mode has been observed by neutron and X-ray scattering experiments.[66,67] The softening in the out-of-plane mode indicates that CaAlSi is on the verge of a structural instability toward the corrugated structure. This is indeed observed as the 5-H and 6-H superstructure for this compound.[60−63] Calculation of the phonon DOS has been studied in detail only for CaAlSi. It is, thus, desired to make a thorough investigation of the phonon DOS for SrGaSi, BaGaSi, and $YbGa_{1.15}Si_{0.85}$, especially of the alkaline-earth involved mode and the out-of-plane mode in the Ga/Si layer, to explain the material dependence of T_C in the MGaSi systems.

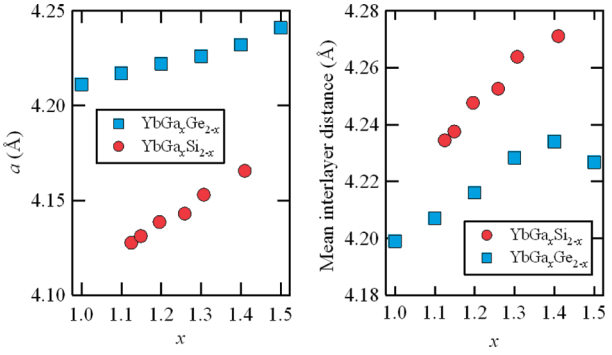

Figure 10. Lattice constant a and the mean interlayer distance for $YbGa_xSi_{2-x}$ and $YbGa_xGe_{2-x}$. The mean interlayer distance corresponds to c for the former and $c/4$ for the latter.

Finally, let us compare the properties of $YbGa_xSi_{2-x}$ with those of YbGaGe. The latter compound has the hexagonal YPtAs-type ($P6_3/mmc$) structure,[68] which is derived from the AlB_2-type structure by a systematic puckering of the Ga−Ge layers to form the 4-fold periodicity in the stacking sequence of the layer along the c axis.[69] YbGaGe does not show superconductivity down to 1.4 K.[70] Yb ion in YbGaGe is also close to divalent. Our previous PFY−XAS study for YbGaGe yielded the mean valence of $Yb^{2.27+}$,[36] and X-ray absorption results gave $Yb^{2.17+}$.[71] The Yb ions are close to divalency in both YbGaGe and $YbGa_xSi_{2-x}$, therefore ruling out the scenario of pair breaking related to the local magnetic moment of Yb to explain the absence of superconductivity in YbGaGe.

To discuss the difference between YbGaGe and $YbGa_xSi_{2-x}$, let us focus on the crystal structure of the two systems. Figure 10 shows the comparison of the lattice constant a and the mean interlayer distance of $YbGa_xSi_{2-x}$ and $YbGa_xGe_{2-x}$. Data for the latter compound are taken from literature.[72] Note that $YbGa_xGe_{2-x}$ has the 4-fold stacking sequence along the c axis as shown in Figure 1c, therefore $c/4$ yields the mean interlayer distance, while for $YbGa_xSi_{2-x}$ the interlayer distance is identical to c. The in-plane lattice constant a is larger for $YbGa_xGe_{2-x}$ than for $YbGa_xSi_{2-x}$ for the whole investigated x range. On the other hand, the mean interlayer distance is shorter in

(59) Evans, M. J.; Wu, Y.; Kranak, V. F.; Newman, N.; Reller, A.; Garcia-Garcia, F. J.; Häussermann, U. *Phys. Rev B* **2009**, *80*, 064514.
(60) Ghosh, A. K.; Tokunaga, M.; Tamegai, T. *Phys. Rev. B* **2003**, *68*, 054507.
(61) Kuroiwa, S.; Sagayama, H.; Kakiuchi, T.; Sawa, H.; Noda, Y.; Akimitsu, J. *Phys. Rev. B* **2006**, *74*, 014517.
(62) Sagayama, H.; Wakabayashi, Y.; Sawa, H.; Kamiyama, T.; Hoshikawa, A.; Harjo, S.; Uozato, K.; Ghosh, A. K.; Tokunaga, M.; Tamegai, T. *J. Phys. Soc. Jpn.* **2006**, *75*, 043713.
(63) Sparta, K. M.; Muller, R.; Merz, M.; Roth, G.; Adelmann, P.; Wolf, T. *Acta Crystallogr., Sect. B* **2006**, *62*, 710.
(64) Calandra, M.; Mauri, F. *Phys. Rev. Lett.* **2005**, *95*, 237002.
(65) Hinks, D. G.; Rosenmann, D.; Claus, H.; Bailey, M. S.; Jorgensen, J. D. *Phys. Rev. B* **2007**, *75*, 014509.
(66) Heid, R.; Bohnen, K. -P.; Renker, B.; Adelmann, P.; Wolf, T.; Ernst, D.; Schober, H. *J. Low Temp. Phys.* **2007**, *147*, 375.
(67) Kuroiwa, S.; Baron, A. Q. R.; Muranaka, T.; Heid, R.; Bohnen, K.-P.; Akimitsu, J. *Phys. Rev. B* **2008**, *77*, 140503(R).
(68) Salvador, J. R.; Guo, F.; Hogan, T.; Kanatzidis, M. G. *Nature* **2003**, *425*, 702.
(69) Hoffmann, R.-D.; Pöttgen, R. *Z. Kristallogr.* **2001**, *216*, 127.
(70) Muro, Y.; Nakagawa, T.; Umeo, K.; Itoh, M.; Suzuki, T.; Takabatake, T. *J. Phys. Soc. Jpn.* **2004**, *73*, 1450.
(71) Booth, C. H.; Christianson, A. D.; Lawrence, J. M.; Pham, L. D.; Lashley, J. C.; Drymiotis, F. R. *Phys. Rev. B* **2007**, *75*, 012301.
(72) Tsujii, N.; Furubayashi, T.; Kitazawa, H.; Kido, G. *J. Alloys Compd.* **2005**, *393*, 41.

$YbGa_xGe_{2-x}$ than in $YbGa_xSi_{2-x}$. In addition, the shortest interlayer Ga−Ga distance in YbGaGe, which is shown as dotted lines in Figure 1 c, is 3.226 Å, whereas the value for $YbGa_{1.15}Si_{0.85}$ corresponds to c = 4.238 Å. These data point to a stronger interlayer coupling in $YbGa_xGe_{2-x}$ than in $YbGa_xSi_{2-x}$. Thus, the interlayer interaction in $YbGa_xGe_{2-x}$ appears to cause a significant difference in the local electronic structure and the phonon density of state between $YbGa_xSi_{2-x}$ and $YbGa_xGe_{2-x}$. It is notable that for C_6Ca the phonon mode of Ca parallel to the honeycomb layer is suggested to be important for superconductivity.[64] If a similar phonon mode of Yb is relevant for superconductivity in $YbGa_xSi_{2-x}$, it is likely that the puckering in the honeycomb layer and the strong interlayer coupling disturb the in-plane vibrations of Yb, resulting in the absence of superconductivity in YbGaGe. This interpretation is supported by the electronic structure calculations for the AlB_2-type EuGaSi and the YPtAs-type EuGaGe.[55,57] The results indicated that the interlayer interactions for the former are predominantly mediated via the Eu 5d band, and the Ga−Si orbital interactions are two-dimensional.[52] On the other hand, the calculation for the latter suggested that the interlayer Ga−Ga interaction is attractive, suggesting more three-dimensional character inside the Ga−Ge sublattice.

Summary

We synthesized polycrystalline samples of $YbGa_xSi_{2-x}$ by arc melting and annealing. XRD and EPMA studies showed that the ternary phase with the AlB_2-type structure exists in the chemical composition range of $1.12(1) \leq x \leq 1.49(3)$. The lattice parameters and volume increase linearly with x. Electrical resistivity and magnetic susceptibility measurements showed superconducting transition with T_C decreasing from 2.4 K for x = 1.15 to 1.8 K for x = 1.31. Electrical resistivity for x = 1.41 also suggested the onset of the superconducting transition to take place just below 1.8 K. The Seebeck coefficient for $x = 1.20$ showed a negative sign below room temperature, suggesting that electrons are major carriers.

PFY−XAS measurements at the Yb L_{III} edge revealed the valence fluctuating state of $Yb^{2.3+}$ for x = 1.2, 1.3, and 1.4. This implies that the 4f orbitals of Yb have a strong hybridization with the d orbitals of Yb and π orbitals of the Ga/Si layer, those of which are considered to be responsible for the superconductivity from the band calculations for other ternary silicide superconductors. No temperature dependence of the valence is observed. The results have been discussed in comparison with those for MGaSi (M = Ca, Sr, Ba) and C_6Ca, which have the same or similar structure. We suggest that the phonon mode including the Yb or M atoms can be relevant for the material dependence of T_C in SrGaSi, BaGaSi, and $YbGa_xSi_{2-x}$. Thus, both electrons and phonons related to Yb are likely to play an essential role for the superconductivity in the $YbGa_xSi_{2-x}$ system. The absence of superconductivity in the related compound YbGaGe has inferred that the two-dimensional character of the Ga/Si layers is essential for the superconductivity in $YbGa_xSi_{2-x}$.

Acknowledgment. This research is supported by the Grant-in-Aid for Scientific Research, 19740221. The PFY−XAS and the RIXS measurements were done at BL15XU, SPring-8 (under Proposal No. 2007B4701), Japan. We thank Yuko Isozaki and Toshiya Ogiwara of Materials Analysis Station, NIMS, for EPMA measurements. We also thank Daisuke Nomoto at BL15XU for the help of X-ray experiments.

Supporting Information Available: Powder X-ray diffraction patterns with Rietveld fitting results for $YbGa_xSi_{2-x}$ annealed samples, results of resonant inelastic X-ray scattering experiments, and specific heat of $YbGa_xSi_{2-x}$ annealed samples at low temperatures (PDF). This material is available free of charge via the Internet at http://pubs.acs.org.